

1
2
3
4
5
6
7
8
9
10
11
12
13
14
15
16
17
18
19
20
21
22
23
24
25
26
27
28
29
30
31
32
33
34
35
36
37
38
39
40
41
42
43
44
45
46

Transcriptional background effects on a tumor driver gene in a transgenic medaka melanoma model

Shahad Abdulsahib¹, William Boswell¹, Mikki Boswell¹, Markita Savage¹, Manfred Schartl^{1,2}, Yuan Lu^{1,*}

¹*Xiphophorus* Genetic Stock Center, Department of Chemistry and Biochemistry, 419 Centennial Hall, Texas State University, San Marcos, TX, USA.

²Developmental Biochemistry, Biozentrum, University of Würzburg, Würzburg, Germany

*Corresponding Author: YUAN LU
Email: y_l54@txstate.edu

47 **Abstract**

48 The *Xiphophorus* melanoma receptor kinase gene, *xmrk*, is a bona fide
49 oncogene driving melanocyte tumorigenesis of *Xiphophorus* fish. When
50 ectopically expressed in medaka, it not only induces development of several
51 pigment cell tumor types in different strains of medaka, but also induces different
52 tumor types within the same animal, suggesting its oncogenic activity has a
53 transcriptomic background effect. Although the central pathways that *xmrk*
54 utilizes to lead to melanomagenesis are well documented, genes and genetic
55 pathways that modulate the oncogenic effect, and alter the course of disease
56 have not been studied so far. To understand how the genetic networks between
57 different histocytes of *xmrk*-driven tumors are composed, we isolated two types
58 of tumors, melanoma and xanthoerythrophoroma, from the same *xmrk* transgenic
59 medaka individuals, established the transcriptional profiles of both *xmrk*-driven
60 tumors, and compared (1) genes that are co-expressed with *xmrk* in both tumor
61 types, and (2) differentially expressed genes and their associated molecular
62 functions, between the two tumor types. Transcriptomic comparisons between
63 the two tumor types show melanoma and xanthoerythrophoroma are
64 characterized by transcriptional features representing varied functions, indicating
65 distinct molecular interactions between the driving oncogene and the cell type-
66 specific transcriptomes. Melanoma tumors exhibited gene signatures that are
67 relevant to proliferation and invasion while xanthoerythrophoroma tumors are
68 characterized by expression profiles related metabolism and DNA repair. We
69 conclude the transcriptomic backgrounds, exemplified by cell-type specific genes
70 that are downstream of *xmrk* effected signaling pathways, contribute the potential
71 to change the course of tumor development and may affect overall tumor
72 outcomes.

74 **Introduction**

75 Efforts in the past few decades to identify major disease driver genes have
76 advanced both our understanding of disease etiology and therapeutic
77 development. The genetic background considerably impacts the phenotype of a
78 specific disease. Individuals carrying the same disease driver can exhibit
79 diverged penetrance and expressivity. These effects are linked to genetic
80 background and/or environmental influence on the causal driver function and can
81 complicate diagnosis and proper treatment [1-4]. We now know that genetic
82 background effects are involved in epistatic interactions modulating disease
83 driver function [5, 6]. However, oncogenicity is not universal in different cell
84 types. Known oncogenes preferentially induce certain types of cancer, e.g., *RAS*
85 for pancreas cancer [7], *MYC* for leukemia [8, 9], *SRC* for sarcomas [10], *EGFR*
86 for squamous cell carcinoma, glioblastomas, lung cancer [11-13], *ERBB2* for
87 breast, salivary gland, and ovarian carcinomas [14, 15]. Although the mechanism
88 of cell transformation initiated by the oncogenes are well studied, how they
89 interact with different cell type-specific transcriptomes is not. Delineating
90 interactions between a driving oncogene and a cell-specific transcriptional
91 environment is important for a full understanding of the function, and cell type
92 specific modulators of oncogene action.

93 Answering the above question, i.e., how oncogenes interact with different
94 transcriptional backgrounds, requires a model system that develops both
95 tractable, and different types of tumors. *Xiphophorus*, a genus of small
96 freshwater fish, is best known for its inter-species hybridization-induced
97 tumorigenesis. It has been shown that a mutant copy of the Epidermal Growth
98 Factor Receptor encoding gene (*egfrb*) named *Xiphophorus* Melanoma Receptor
99 Kinase (*xmrk*) is an oncogene driving tumor development. When this natural
100 mutant gene loses its unlinked regulator following interspecies hybridization due
101 to Mendelian segregation, the *xmrk* overexpresses. It drives tumorigenesis of
102 macromelanophores, a nevus-type of pigment cells in fish. In addition, its level of
103 overexpression correlates with malignancy. Both the histology, and
104 transcriptional features of these pigment cell tumors are similar to human
105 melanoma [16-19]. When the *xmrk* gene is ectopically expressed under a
106 universal promoter in Japanese medaka, a closely related species to
107 *Xiphophorus*, all embryonic cell types underwent dysregulated proliferation and
108 eventually led to embryo death. However, under regulation of the pigment cell-
109 specific *mitfa* promoter, *xmrk* drives several types of pigment cell-specific
110 tumorigenesis. Using the transcriptional signatures that hallmark the *xmrk*-driven
111 tumor, we have developed a platform utilizing gene expression patterns as a
112 phenotype to assess and score anti-cancer drug candidates to perform mid- to
113 high-throughput phenotype drug screening to forward promising chemical lead-
114 structures for further development [20].

115 Of note, the *xmrk* gene exhibits strong genetic background-dependent
116 tumor phenotypes, as well as diverged tumors from different cell types in the
117 transgenic model: the phenotypes range from xanthoerythrophoromas,
118 extracutaneous melanoma, uveal melanoma in *Carbio* strain;
119 xanthoerythrophoromas, and additional nodular and invasive melanoma in *CabR*
120 strain; extracutaneous melanoma and rarely xanthoerythrophoromas in *HB32C*
121 strain; as well as xanthophore-hyperpigmentation, weakly pigmented melanoma
122 from intestine, and eye melanoma in albino *i-3* strain. The cell types that give rise
123 to these tumors (e.g., dermal and extracutaneous melanocytes for melanoma,
124 xanthophores and erythrophores for xanthoerythrophoromas, uvea pigment cells
125 for eye melanoma) are divergent descendants of neural crest cells. This feature
126 (i.e., different tumor type in the same animal) allows for the identification of
127 shared and diverged gene expression patterns associated with different cell
128 lineages, and to characterize oncogene-transcriptome background interactors
129 (e.g., tumor modifiers) that alter the phenotype of a single driving oncogene.
130 Therefore, the medaka *xmrk* transgenic model is optimal for studying the
131 question of transcriptional cell-type specific background effect on oncogenes.

132 Herein, we performed transcriptome profiling of xanthoerythrophoroma
133 and melanoma tumors isolated from the same animals, compared gene
134 expression of the same tumor type among different individuals, and investigated
135 transcriptional differences between tumor types, in order to: 1. Characterize the
136 tumor cell transcriptome to identify the genes that form a network with a single
137 driver oncogene; 2. Investigate transcriptional signatures that differentiate the

138 *xmrk*-driven phenotypes in distinct cell types exhibiting potential diverged
139 transcriptional environments.

140

141 **Materials and Methods**

142 **Fish utilized**

143 Seven twelve-month old male *mitf:xmrk*-transgenic (*tg-mel*) from the
144 *Carbio* strain were raised and maintained in the *Xiphophorus* Genetic Stock
145 Center in accordance with the Institutional Animal Care and Use Committee
146 (IACUC) protocol (IACUC20173294956). Texas State University has an Animal
147 Welfare Assurance on file (#A4147) with the Office of Laboratory Animal Welfare
148 (OLAW), National Institute of Health.

149

150 **RNA isolation**

151 The *tg-mel* medaka were anesthetized by hypothermia, sacrificed,
152 followed by isolation of both melanoma and xanthoerythrophoroma tumors.
153 Tumor samples were immediately placed in 1.5 mL microcentrifuge tubes
154 containing 300 μ L TRI Reagent (Sigma Inc., St. Louis, MO, USA) followed by
155 homogenization with a tissue homogenizer. After the initial homogenization, 300
156 μ L of fresh TRI Reagent and 120 μ L of chloroform were added to the 1.5 mL
157 microcentrifuge tube and shaken vigorously for 15 sec. Phase separation was
158 performed by centrifugation (12,000 x g for 5 min at 4°C). The aqueous phase
159 was then added to a new 1.5 mL microcentrifuge tube and an additional
160 chloroform extraction was performed (300 μ L TRI Reagent, 60 μ L chloroform).
161 Following extraction, the nucleic acids were precipitated with 500 μ L of 70%
162 EtOH and transferred to a Qiagen RNeasy mini spin column. DNase treatment
163 was performed on-column for 15 min at 25°C, and RNA samples were
164 subsequently eluted with 100 μ L RNase-free water. RNA concentrations were
165 quantified with a Qubit 2.0 fluorometer (Life Technologies, Grand Island, NY,
166 USA), and RNA quality was assessed based on RNA integrity (RIN) score with
167 an Agilent 2100 Bioanalyzer (Agilent Technologies, Santa Clara, CA, USA).

168

169 **Transcriptional profiling of tumors**

170 All samples sequenced had an RNA Integrity (RIN) score \geq 8.0. Individual
171 sequencing libraries were constructed using the Illumina TruSeq mRNA Library
172 Prep Kit with polyA selection, and libraries were sequenced (150 bp, paired-end
173 [PE] reads) on the Illumina HiSeq 2000 platform. Raw sequencing reads were
174 subsequently processed using fastx_toolkit for sequencing adaptor removal, low
175 quality base calls, and removal of low-quality sequencing reads,

176 Processed sequencing reads were mapped to the medaka reference
177 genome (Ensembl release 85, ftp://ftp.ensembl.org/pub/release-85/fasta/oryzias_latipes/dna/) using Tophat2 [21]. Gene expression was
178 quantified using SubReads package function FeatureCounts [22]. Processed
179 read counts per gene are listed in Table S5.

180

181 **Principle component analysis and gene co-expression analyses**

182

183 Gene expression read counts of each sample were normalized to
184 corresponding library size and transcript lengths, and converted to Reads count
185 per Kilobase per Million reads (rpkm). Principle Component Analysis (PCA) was
186 performed using the R package “prcomp” using the scaled rpkm of all samples.
187 Spearman ranking correlation was performed using R programming “cor”
188 function. For each tumor type, samples are ranked based on the *xmrk* expression
189 level. The rpkm values of each gene were subsequently ordered in the ranked
190 samples. A correlation coefficient was subsequently calculated between the gene
191 and *xmrk*. Correlation coefficients > 0.9 or < -0.9 were considered a strong
192 correlation; coefficients between -0.19 and 0.19 were considered no correlation.
193

194 **Differentially expressed genes between tumor types**

195 Differentially Expressed Genes (DEGs) between tumor types were
196 identified using R/Bioconductor package edgeR [23]. The \log_2 Fold Change
197 (\log_2 FC) was calculated using melanoma tumors as control samples. The Area
198 Under Curve (AUC) of the Receiver Operating Characteristic (ROC) curve was
199 calculated to assess true and false positive rates for each gene tested by the R
200 package pROC. A set of statistical thresholds was applied to define DEGs:
201 \log_2 FC ≥ 1 or ≤ -1 (\log_2 FC ≥ 1 means a gene is higher expressed in
202 xanthoerythrophoromas tumors; \log_2 FC ≤ -1 means a gene is higher express in
203 melanoma tumors), \log_2 CPM differences ≥ 1 , False Discovery Rate (FDR) ≤ 0.05
204 and ROC curve AUC = 1.
205

206 **Functional analyses of genes**

207 Reciprocal Best Hits (RBH) between human orthologs of medaka genes
208 were identified using Blast and subsequently utilized to find human orthologs of
209 medaka genes that co-expressed with *xmrk* or differentially expressed between
210 different tumor types. Gene Set Enrichment Analyses (GSEA) was performed
211 using GSEA tool package in Bioconductor [24, 25]. Medaka datasets were
212 queried against datasets collected in GSEA database. Ingenuity Pathway
213 Analyses (IPA, Qiagen, Redwood City, CA) was used for functional specificity
214 analysis. The goal of these analyses was to identify the biological functions of the
215 *xmrk*-co-expressed genes and inter-tumor type DEGs, therefore, default over-
216 representation analyses was not applied. Genes that were not included and
217 analyzed by either software were manually curated using GeneCard suite [26]
218 and published literature.
219

220 **Results**

221 **Tumor type-specific gene co-expression with *xmrk***

222 Principle Component Analyses (PCA) showed melanoma and
223 xanthoerythrophoromas tumor samples are separated, with the tumor type being
224 the driving dimension that separates the gene expression profiles of all tumor
225 samples (Fig. S1). Genes that are positively or negatively correlated with *xmrk*
226 expression patterns were identified using Pearson correlation in both tumor
227 types. There are 17 genes that are co-expressed with *xmrk* in both tumor types
228 (Fig. 1a; Table S1); 14 genes co-expressed with *xmrk* only in melanoma tumors

229 (Fig. 1b; Table S2); and 29 genes co-expressed with *xmrk* only in
230 xanthoerythrophoroma tumors (Fig. 1c; Table S3). Genes that are co-expressed
231 with *xmrk* in both tumor types are mainly associated with differentiation (*Inx1*,
232 *Inx2b*, *pdlim5b* and *sema4b*), proliferation (*dyrk3*, *egfra*, *plpp1*), cell cycle
233 regulation (*Ilgl2*), and cell-microenvironment interaction (*itgb3a*). These genes
234 and related molecular functions represent universal *xmrk* activities regardless of
235 cell types (Fig. 1a; Table S1).

236 In contrast, genes that are co-expressed with *xmrk* exclusively in
237 melanoma tumors are associated with apoptosis (*aifm2*), immune response
238 (*abhd12* and *pmse2*), metabolism (*enosf1*), metastasis (*mtss1la*), pigmentation
239 (*crhbp*), proliferation (*I3mbtl2*) and vesicle trafficking [*vps18*; (Fig. 1b; Table S2)].
240 Genes that co-expressed with *xmrk* only in xanthoerythrophoroma tumors are
241 associated with cell cycle (*ankle2*, *ccng1*), cell-microenvironment interaction
242 (*gsna*), chromosome integrity (*tp53rk*), differentiation (*rxf3*, *tefa* and *znrf3*), DNA
243 repair (*telomerase*), fatty acid transportation, metabolism and lipid homeostasis
244 (*lonp2*, *scdb*, *fabp11a* and *mbtps1*), mitochondrial function (*mrpl15*, *mrpl30*,
245 *mrps17* and *mrps26*), nucleotide metabolism (*nudt16*), proliferation (*rassf1*),
246 transport (*scnm1*), and signaling regulation [*vps4b* and *vta1*; (Fig. 1c; Table S3)].

247

248 **Gene expression pattern differentiating tumor types**

249 We assessed differentially expressed genes between melanoma and
250 xanthoerythrophoroma tumors to assess cellular functional differences between
251 the two tumor types. There are 119 genes highly expressed in melanoma tumors,
252 and 63 genes highly expressed in the xanthoerythrophoroma tumors (Fig. 2;
253 Table S4). As expected, genes belonging to pathways associated with eumelanin
254 production are highly expressed in melanoma tumors. We also identified
255 functions of 77 genes that are associated with cell-microenvironment
256 interactions, differentiation, proliferation, metabolism, dopamine homeostasis,
257 immune response and PPAR/RXR activation. All proliferation related genes, and
258 a majority of genes associated with differentiation, and cell-microenvironment
259 related are higher expressed in melanoma tumors than xanthoerythrophoromas
260 (Fig. 3).

261

262 **Discussion**

263 The *xmrk* is a bona fide oncogene. It is a duplicated mutant *egfr* copy in a
264 few species belonging to the Central American fish genus *Xiphophorus*, and it
265 drives spontaneous tumorigenesis in interspecies *Xiphophorus* hybrids due to
266 negative epistasis. Functional studies on *xmrk* ectopically expressed in-vitro in
267 murine cells or in transgenic zebrafish and medaka, revealed it drives
268 dedifferentiation, enhanced proliferation, and tumorigenesis [27-30]. Combined
269 with tumor transcriptome, the tumor phenotypical differences allow for the
270 deconvolution of transcriptional networks that interact with *xmrk* to modify its
271 function. The *xmrk* is constitutively active independent of EGF binding, due to
272 mutation induced dimerization [31]. Since human EGFR is associated to a
273 majority types of human cancers, characterizing its modifiers is important in fully

274 understanding its mode of action, and overcoming current therapeutic resistance
275 to anti-EGFR compounds.

276 The recurrent somatic mutations in tumor cells affect almost every level of
277 transcriptional control (e.g., cellular signaling pathways, transcription factors,
278 enhancer, chromatin structure) [32-39]. Oncogenes can disrupt normal gene
279 expression regulatory mechanisms and transform normal cells into cancer cells.
280 Even though tumorigenesis is a multi-step process, oncogene expression can be
281 indispensable for cancer cell proliferation even the cancer cells have progressed
282 long after a neoplastic state. This proliferative reliance on oncogene expression
283 is named oncogene transcriptional addiction [32, 40]. Studies of *xmrk*-driven
284 tumors in both *Xiphophorus* and transgenic medaka showed tumor cells exhibit
285 high levels of *xmrk* expression [29, 41]. The *xmrk*-driven cancer can be observed
286 4 weeks following hatching in *xmrk*-medaka. The fish utilized in this study are
287 one-year old with advanced stage tumors, suggesting the tumor cells are
288 addicted to *xmrk* expression, and the transcriptome of the cancer cells is still
289 directly under master regulation of *xmrk* despite exhaustion of *xmrk*'s initial
290 neoplasm triggering activity.

291 The medaka transgenic system enables investigation of how *xmrk*
292 interacts with transcriptomes of different cell lineages, and characterize cell type-
293 specific genes interactions. Using the *xmrk*-transgenic medaka system, we
294 sought to answer two questions: 1. How are the genetic networks under *xmrk*
295 regulation different between the two tumor types that are driven by the same
296 oncogene; 2. How are the transcriptional phenotypes different between tumor
297 types as a result of driving oncogene *xmrk* interaction with the cell type specific
298 transcriptional landscape.

299 To answer the first question, we compared genes that co-expressed with
300 *xmrk* in both melanoma and xanthoerythrophoroma tumors. Although *xmrk* drives
301 proliferation, cell-microenvironment interaction, cell cycle and differentiation in
302 both tumor types, the observation of varied genetic functions that are associated
303 with genes that co-expressed with *xmrk* in a tumor type-specific way is
304 suggestive that *xmrk* regulate different cellular processes between melanoma
305 and xanthoerythrophoroma tumor cells.

306 To answer the second question, we compared bulk transcriptomic
307 differences between the melanoma and xanthoerythrophoroma tumors. In
308 consistence with the distinguished coloration between the two tumor types,
309 genes associated with pigmentation pathways are observed. Differentiation
310 related genes are also a reflection of cell type difference between the two tumor
311 types. However, presence of pivotal differentiation genes (33 genes; Fig. 3)
312 suggest the two tumor types may be at varied differentiation stages or potential.
313 Genes related to proliferation and cell-microenvironment interactions are
314 predominantly highly expressed in melanoma tumors. These include a few proto-
315 oncogenes like endothelin receptor *ednrbb*, sarcoma viral oncogene homolog
316 *kita*, Ras like estrogen regulated growth factor *reg*, pleiotrophin *ptn*, FYN proto-
317 oncogene *fyna*, erbb2 receptor tyrosine kinase 3b *erbb3b*. This evidence, along
318 with previous observation that melanotic tumors are highly invasive into
319 musculature and internal organs while xanthoerythrophoromas grow more as

320 epiphytic nodules [42], suggests the melanoma tumors are more proliferative
321 than xanthoerythrophoromas. Some of these proto-oncogenes are known to be
322 induced by *xmrk* in *Xiphophorus* [43-46], culture murine cells, and most of them
323 were reported to be involved in human melanomagenesis [43, 47-52]. For
324 example, the *fyna* mouse ortholog (Fyn) has been shown to play an important
325 role in *xmrk* signal transduction at protein and post-translational level [19]. Herein
326 this study we confirm the activity is also displayed at transcriptional level. It is
327 also important to note that fibronectins *fn1b*, integrin *itga11a*, laminin *lama4*,
328 cadherin *cdh6*, collagens *col11a1a*, *col5a3b*, *col4a5*, *col12a1b*, *col4a6* *col5a2*,
329 matrix metalloproteinase *mmp16*, ADAMs *adamts16* and *adamts12* are also
330 highly expressed in the melanoma tumors. These genes are reliable markers for
331 tumor cell invasion and metastasis. For example, *col4a5* encodes collagen that
332 make up basement membrane that are involved in metastasis [53]; *cdh6* involves
333 in epithelial-mesenchymal transition [54, 55]; *mmp16* promotes tumor metastasis
334 [56]. Combining this observation with the highly expressed proto-oncogenes
335 suggests the melanoma tumors exhibit a higher potential to invasion.

336 In summary, genes that are co-expressed with *xmrk* in melanoma and
337 xanthoerythrophoroma tumors, and differentially expressed genes between the
338 two tumor types are involved in diverged biological functions as a result of
339 distinct molecular interactions between the driving oncogene and cell type
340 specific modifiers. We conclude *xmrk* oncogene exhibits a strong transcriptomic
341 background dependent activity. The oncogene modifiers can change the course
342 of tumor development and may affect overall tumor outcomes.

343 344 **Acknowledgements**

345 This work was supported by National Institutes of Health grant R24-OD-
346 011120, and R15-CA-223964.

347 348 **Figure Legend**

349 **Figure 1. Co-expressed genes of the *xmrk* in melanoma and**
350 **xanthoerythrophoroma tumors** Genes that exhibit positive or negative
351 correlation to *xmrk* expression in (a) both tumor types, (b) only in melanoma
352 tumors and (c) only in xanthoerythrophoroma tumors are shown. Solid lines
353 represent scaled mean gene expression. Upper and lower boundaries of the
354 shaded areas indicate the max and minimum expression levels respectively.

355
356 **Figure 2. Differentially expressed genes between melanoma and**
357 **xanthoerythrophoroma tumors** Differentially expressed genes are identified
358 between melanoma and xanthoerythrophoroma tumors. There are 119 genes
359 highly expressed in the melanoma tumors, and 63 genes highly expressed in the
360 xanthoerythrophoroma tumors. Volcano plot shows \log_2FC between tumor types,
361 and $-\log_{10}FDR$ of differential expression test. Red dots highlight differentially
362 expressed genes, gray dots are genes that are not differentially expressed.

363
364 **Figure 3. Functional categories of differentially expressed genes between**
365 **tumor types** Functions of inter-tumor type differentially expressed genes are

366 shown. Colored blocks represent functional categories. Black arrows mean a
367 specific gene over expressed in melanoma, and orange arrows mean a gene
368 over expressed in xanthoerythrophoroma tumors, with the numbers indicated
369 Log₂FC of the relative gene expression.

370

371 **Supplement Table S1. Genes exhibiting positive or negative correlation to**
372 ***xmrk* expression in both tumor types**

373

374 **Supplement Table S2. Genes exhibiting positive or negative correlation to**
375 ***xmrk* expression only in melanoma tumors**

376

377 **Supplement Table S3. Genes exhibiting positive or negative correlation to**
378 ***xmrk* expression only in xanthoerythrophoroma tumors**

379

380 **Supplement Table S4. Differentially expressed genes between melanoma**
381 **and xanthoerythrophoroma tumors**

382

383 **Supplement Table S5. RPKM values of gene expression**

384

385 **Supplement Figure**

386 **Figure S1. Principle component analyses of gene expression profiles**

387 Scatter plot showing distribution of samples distribution on principle component
388 (PC) 1 & 2. Black square dots represent melanoma tumors, and orange square
389 dots represent xanthoerythrophoroma tumors.

390

391 **Additional Information:**

392 The authors have no competing interests, or other interests that might be
393 perceived to influence the results and/or discussion reported in this paper.

394

395 **Data availability statement:**

396 The raw sequencing files are deposited in Gene Expression Omnibus. The
397 accession number will be publicly available upon manuscript acceptance for
398 publication.

399

400 **References:**

401

- 402 1. Hou, J., et al., *Complex modifier landscape underlying genetic background*
403 *effects*. Proc Natl Acad Sci U S A, 2019. **116**(11): p. 5045-5054.
- 404 2. Hou, J., et al., *Genetic Network Complexity Shapes Background-*
405 *Dependent Phenotypic Expression*. Trends Genet, 2018. **34**(8): p. 578-
406 586.
- 407 3. Chandler, C.H., et al., *Causes and consequences of genetic background*
408 *effects illuminated by integrative genomic analysis*. Genetics, 2014.
409 **196**(4): p. 1321-36.

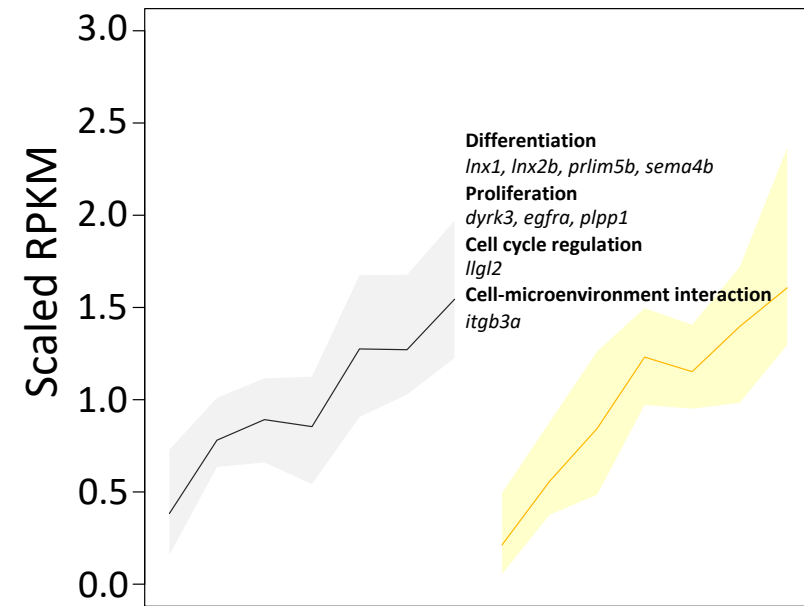
- 410 4. Cooper, D.N., et al., *Where genotype is not predictive of phenotype:*
411 *towards an understanding of the molecular basis of reduced penetrance in*
412 *human inherited disease.* Hum Genet, 2013. **132**(10): p. 1077-130.
- 413 5. Mackay, T.F. and J.H. Moore, *Why epistasis is important for tackling*
414 *complex human disease genetics.* Genome Med, 2014. **6**(6): p. 124.
- 415 6. Phillips, P.C., *Epistasis--the essential role of gene interactions in the*
416 *structure and evolution of genetic systems.* Nat Rev Genet, 2008. **9**(11): p.
417 855-67.
- 418 7. RW, R., *Cancer Biology.* 1995, New York: Oxford University Press.
- 419 8. Fatma, H. and H.R. Siddique, *Role of long non-coding RNAs and MYC*
420 *interaction in cancer metastasis: A possible target for therapeutic*
421 *intervention.* Toxicol Appl Pharmacol, 2020. **399**: p. 115056.
- 422 9. Baluapuri, A., E. Wolf, and M. Eilers, *Target gene-independent functions*
423 *of MYC oncoproteins.* Nat Rev Mol Cell Biol, 2020. **21**(5): p. 255-267.
- 424 10. G., C., *Oncogenes.* 1995: Jones and Bartlett Publishers.
- 425 11. Boeckmann, L., M.C. Martens, and S. Emmert, *Molecular Biology of Basal*
426 *and Squamous Cell Carcinomas.* Adv Exp Med Biol, 2020. **1268**: p. 171-
427 191.
- 428 12. Velazquez, A.I. and C.E. McCoach, *Tumor evolution in epidermal growth*
429 *factor receptor mutated non-small cell lung cancer.* J Thorac Dis, 2020.
430 **12**(5): p. 2896-2909.
- 431 13. Rutkowska, A., et al., *EGFR(vIII): An Oncogene with Ambiguous Role.* J
432 Oncol, 2019. **2019**: p. 1092587.
- 433 14. Kreutzfeldt, J., et al., *The trastuzumab era: current and upcoming targeted*
434 *HER2+ breast cancer therapies.* Am J Cancer Res, 2020. **10**(4): p. 1045-
435 1067.
- 436 15. Robichaux, J.P., et al., *Pan-Cancer Landscape and Analysis of ERBB2*
437 *Mutations Identifies Pozitotinib as a Clinically Active Inhibitor and Enhancer*
438 *of T-DM1 Activity.* Cancer Cell, 2019. **36**(4): p. 444-457 e7.
- 439 16. Lu, Y., et al., *Comparison of Xiphophorus and human melanoma*
440 *transcriptomes reveals conserved pathway interactions.* Pigment Cell
441 Melanoma Res, 2018. **31**(4): p. 496-508.
- 442 17. Meierjohann, S. and M. Scharl, *From Mendelian to molecular genetics:*
443 *the Xiphophorus melanoma model.* Trends Genet, 2006. **22**(12): p. 654-
444 61.
- 445 18. Kazianis, S., et al., *Genetic analysis of neoplasia induced by N-nitroso-N-*
446 *methylurea in Xiphophorus hybrid fish.* Mar Biotechnol (NY), 2001.
447 **3**(Supplement 1): p. S37-43.
- 448 19. Morcinek, J.C., et al., *Activation of STAT5 triggers proliferation and*
449 *contributes to anti-apoptotic signalling mediated by the oncogenic Xmrk*
450 *kinase.* Oncogene, 2002. **21**(11): p. 1668-78.
- 451 20. Lu, Y., et al., *Application of the Transcriptional Disease Signature (TDSs)*
452 *to Screen Melanoma-Effective Compounds in a Small Fish Model.* Sci
453 Rep, 2019. **9**(1): p. 530.

- 454 21. Kim, D., et al., *TopHat2: accurate alignment of transcriptomes in the*
455 *presence of insertions, deletions and gene fusions*. *Genome Biol*, 2013.
456 **14**(4): p. R36.
- 457 22. Liao, Y., G.K. Smyth, and W. Shi, *featureCounts: an efficient general*
458 *purpose program for assigning sequence reads to genomic features*.
459 *Bioinformatics*, 2014. **30**(7): p. 923-30.
- 460 23. Robinson, M.D., D.J. McCarthy, and G.K. Smyth, *edgeR: a Bioconductor*
461 *package for differential expression analysis of digital gene expression*
462 *data*. *Bioinformatics*, 2010. **26**(1): p. 139-40.
- 463 24. Subramanian, A., et al., *Gene set enrichment analysis: a knowledge-*
464 *based approach for interpreting genome-wide expression profiles*. *Proc*
465 *Natl Acad Sci U S A*, 2005. **102**(43): p. 15545-50.
- 466 25. Mootha, V.K., et al., *PGC-1alpha-responsive genes involved in oxidative*
467 *phosphorylation are coordinately downregulated in human diabetes*. *Nat*
468 *Genet*, 2003. **34**(3): p. 267-73.
- 469 26. Stelzer, G., et al., *The GeneCards Suite: From Gene Data Mining to*
470 *Disease Genome Sequence Analyses*. *Curr Protoc Bioinformatics*, 2016.
471 **54**: p. 1 30 1-1 30 33.
- 472 27. Zheng, W., et al., *Xmrk, kras and myc transgenic zebrafish liver cancer*
473 *models share molecular signatures with subsets of human hepatocellular*
474 *carcinoma*. *PLoS One*, 2014. **9**(3): p. e91179.
- 475 28. Li, Z., et al., *Inducible and repressable oncogene-addicted hepatocellular*
476 *carcinoma in Tet-on xmrk transgenic zebrafish*. *J Hepatol*, 2012. **56**(2): p.
477 419-25.
- 478 29. Schartl, M., et al., *A mutated EGFR is sufficient to induce malignant*
479 *melanoma with genetic background-dependent histopathologies*. *J Invest*
480 *Dermatol*, 2010. **130**(1): p. 249-58.
- 481 30. Wellbrock, C., et al., *Signalling by the oncogenic receptor tyrosine kinase*
482 *Xmrk leads to activation of STAT5 in Xiphophorus melanoma*. *Oncogene*,
483 1998. **16**(23): p. 3047-56.
- 484 31. Meierjohann, S., et al., *A structural model of the extracellular domain of*
485 *the oncogenic EGFR variant Xmrk*. *Zebrafish*, 2006. **3**(3): p. 359-69.
- 486 32. Bradner, J.E., D. Hnisz, and R.A. Young, *Transcriptional Addiction in*
487 *Cancer*. *Cell*, 2017. **168**(4): p. 629-643.
- 488 33. Sur, I. and J. Taipale, *The role of enhancers in cancer*. *Nat Rev Cancer*,
489 2016. **16**(8): p. 483-93.
- 490 34. Lawrence, M.S., et al., *Discovery and saturation analysis of cancer genes*
491 *across 21 tumour types*. *Nature*, 2014. **505**(7484): p. 495-501.
- 492 35. Kandoth, C., et al., *Mutational landscape and significance across 12 major*
493 *cancer types*. *Nature*, 2013. **502**(7471): p. 333-339.
- 494 36. Watson, I.R., et al., *Emerging patterns of somatic mutations in cancer*. *Nat*
495 *Rev Genet*, 2013. **14**(10): p. 703-18.
- 496 37. Garraway, L.A. and E.S. Lander, *Lessons from the cancer genome*. *Cell*,
497 2013. **153**(1): p. 17-37.
- 498 38. Vogelstein, B., et al., *Cancer genome landscapes*. *Science*, 2013.
499 **339**(6127): p. 1546-58.

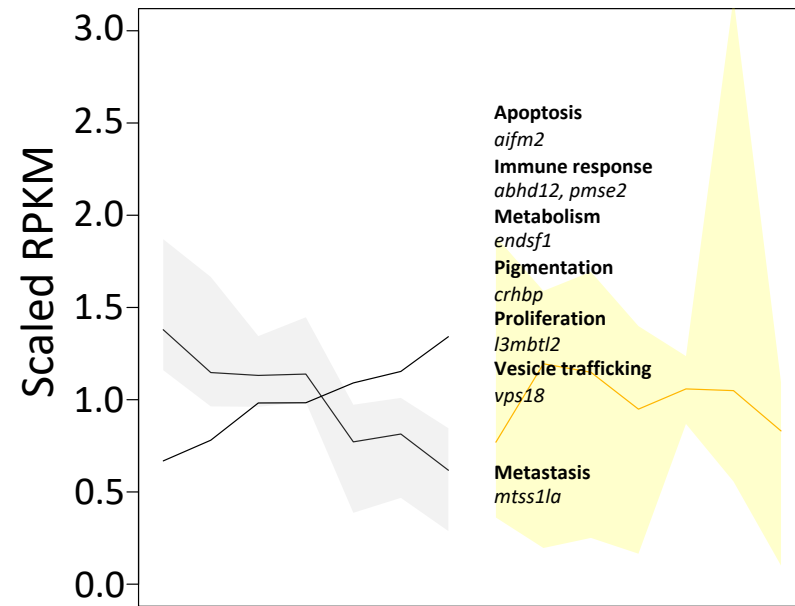
- 500 39. Stratton, M.R., P.J. Campbell, and P.A. Futreal, *The cancer genome*.
501 Nature, 2009. **458**(7239): p. 719-24.
- 502 40. Weinstein, I.B. and A.K. Joe, *Mechanisms of disease: Oncogene*
503 *addiction--a rationale for molecular targeting in cancer therapy*. Nat Clin
504 Pract Oncol, 2006. **3**(8): p. 448-57.
- 505 41. Regneri, J. and M. Scharl, *Expression regulation triggers oncogenicity of*
506 *xmrk alleles in the Xiphophorus melanoma system*. Comp Biochem
507 Physiol C Toxicol Pharmacol, 2012. **155**(1): p. 71-80.
- 508 42. Sugiyama, A., M. Scharl, and K. Naruse, *Histopathologic features of*
509 *melanocytic tumors in Xiphophorus melanoma receptor kinase (xmrk)-*
510 *transgenic medaka (Oryzias latipes)*. J Toxicol Pathol, 2019. **32**(2): p. 111-
511 117.
- 512 43. Lu, Y., et al., *Molecular genetic response of Xiphophorus maculatus-X.*
513 *couchianus interspecies hybrid skin to UVB exposure*. Comp Biochem
514 Physiol C Toxicol Pharmacol, 2015. **178**: p. 86-92.
- 515 44. Schaafhausen, M.K., et al., *Tumor angiogenesis is caused by single*
516 *melanoma cells in a manner dependent on reactive oxygen species and*
517 *NF-kappaB*. J Cell Sci, 2013. **126**(Pt 17): p. 3862-72.
- 518 45. Wellbrock, C., et al., *Activation of p59(Fyn) leads to melanocyte*
519 *dedifferentiation by influencing MKP-1-regulated mitogen-activated protein*
520 *kinase signaling*. J Biol Chem, 2002. **277**(8): p. 6443-54.
- 521 46. Wellbrock, C. and M. Scharl, *Activation of phosphatidylinositol 3-kinase*
522 *by a complex of p59fyn and the receptor tyrosine kinase Xmrk is involved*
523 *in malignant transformation of pigment cells*. Eur J Biochem, 2000.
524 **267**(12): p. 3513-22.
- 525 47. Gottesdiener, L.S., et al., *Rates of ERBB2 Alterations across Melanoma*
526 *Subtypes and a Complete Response to Trastuzumab Emtansine in an*
527 *ERBB2-Amplified Acral Melanoma*. Clin Cancer Res, 2018. **24**(23): p.
528 5815-5819.
- 529 48. Ryu, B., et al., *Comprehensive expression profiling of tumor cell lines*
530 *identifies molecular signatures of melanoma progression*. PLoS One,
531 2007. **2**(7): p. e594.
- 532 49. Garraway, L.A., et al., *Integrative genomic analyses identify MITF as a*
533 *lineage survival oncogene amplified in malignant melanoma*. Nature,
534 2005. **436**(7047): p. 117-22.
- 535 50. Bittner, M., et al., *Molecular classification of cutaneous malignant*
536 *melanoma by gene expression profiling*. Nature, 2000. **406**(6795): p. 536-
537 40.
- 538 51. Ross, D.T., et al., *Systematic variation in gene expression patterns in*
539 *human cancer cell lines*. Nat Genet, 2000. **24**(3): p. 227-35.
- 540 52. Natali, P.G., et al., *Progression of human cutaneous melanoma is*
541 *associated with loss of expression of c-kit proto-oncogene receptor*. Int J
542 Cancer, 1992. **52**(2): p. 197-201.
- 543 53. Tanjore, H. and R. Kalluri, *The role of type IV collagen and basement*
544 *membranes in cancer progression and metastasis*. Am J Pathol, 2006.
545 **168**(3): p. 715-7.

- 546 54. Gugnani, M., et al., *Cadherin-6 promotes EMT and cancer metastasis by*
547 *restraining autophagy*. *Oncogene*, 2017. **36**(5): p. 667-677.
- 548 55. Clay, M.R. and M.C. Halloran, *Cadherin 6 promotes neural crest cell*
549 *detachment via F-actin regulation and influences active Rho distribution*
550 *during epithelial-to-mesenchymal transition*. *Development*, 2014. **141**(12):
551 p. 2506-15.
- 552 56. Shen, Z., et al., *MMP16 promotes tumor metastasis and indicates poor*
553 *prognosis in hepatocellular carcinoma*. *Oncotarget*, 2017. **8**(42): p. 72197-
554 72204.
555

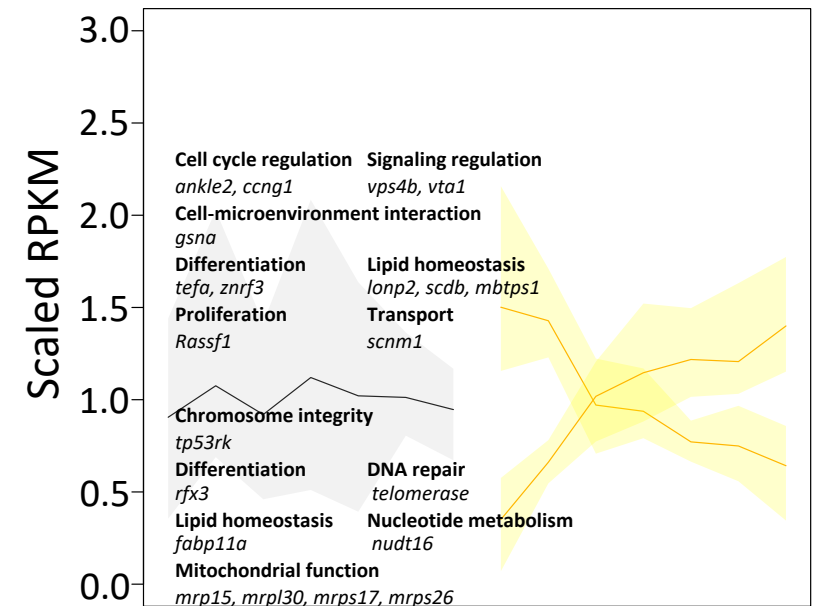
(a)

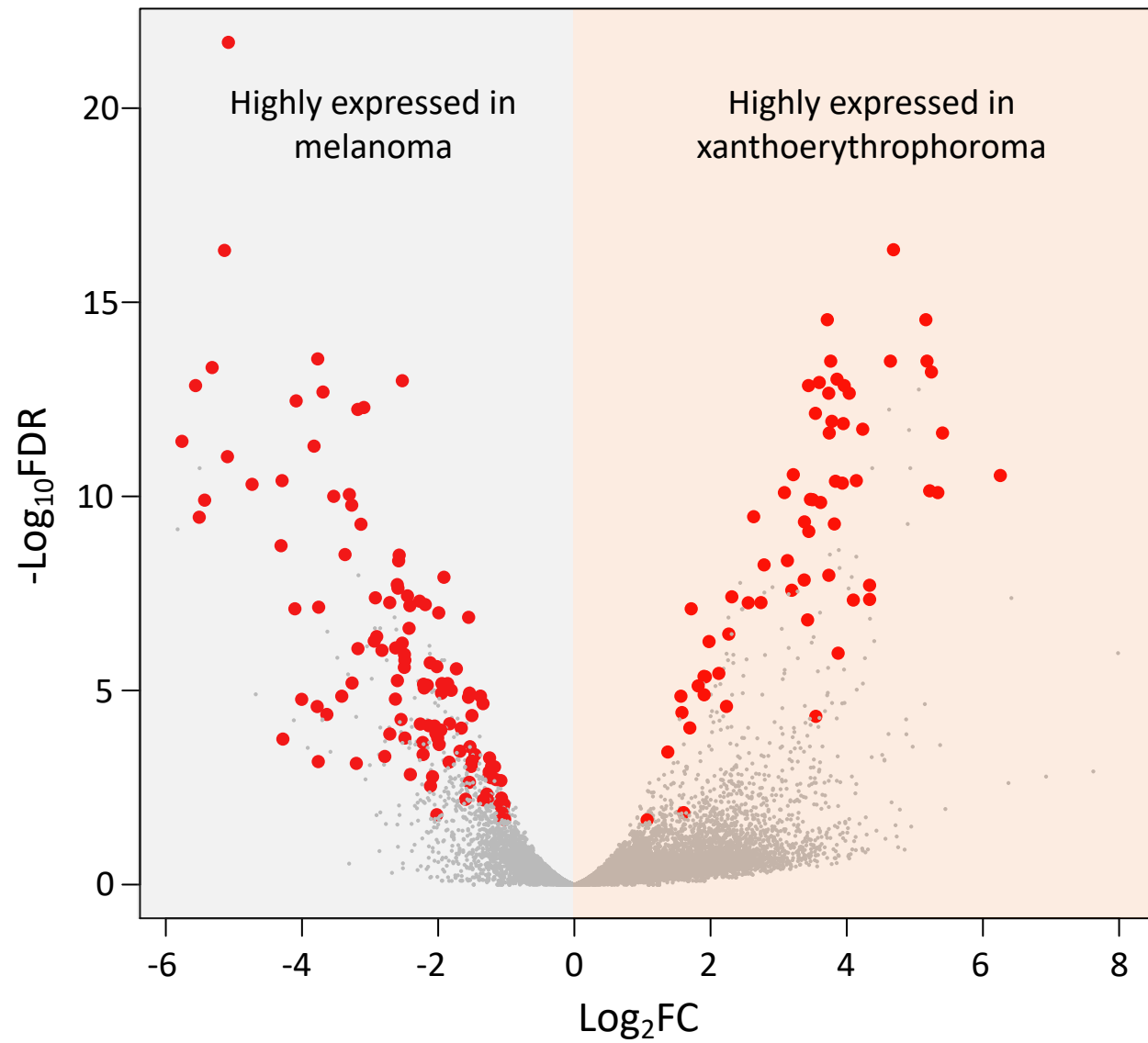


(b)



(c)





Gene Name	logFC	Gene Name	logFC	Gene Name	logFC
<i>tyrp1a</i>	↑ 5.8	<i>ncam2</i>	↑ 4.3	<i>ednrbb</i>	↑ 4.3
<i>slc24a5</i>	↑ 5.6	<i>kita</i>	↑ 3.8	<i>slc39a10</i>	↑ 3.5
<i>dct</i>	↑ 5.5	<i>sall3a</i>	↑ 3.4	<i>relt</i>	↑ 2.7
<i>tyrp1b</i>	↑ 5.4	<i>hoxa13b</i>	↑ 3.2	<i>lmna</i>	↑ 2.3
<i>tyr</i>	↑ 5.3	<i>ppp3ca</i>	↑ 2.9	<i>rap2a</i>	↑ 1.9
<i>col11a1a</i>	↑ 3.3	<i>spon2a</i>	↑ 2.6	<i>fgfr1</i>	↑ 1.8
<i>map6a</i>	↑ 2.9	<i>sost</i>	↑ 2.6	<i>regr</i>	↑ 1.5
<i>thbs4b</i>	↑ 2.8	<i>ntn1b</i>	↑ 2.5	<i>ptn</i>	↑ 1.5
<i>fn1b</i>	↑ 2.7	<i>dlx1a</i>	↑ 2.2	<i>fyna</i>	↑ 1.4
<i>kif1ab</i>	↑ 2.6	<i>bmp7a</i>	↑ 2.2	<i>pamr1</i>	↑ 1.3
<i>itga11a</i>	↑ 2.6	<i>sema5ba</i>	↑ 2.2	<i>s1pr3</i>	↑ 1.3
<i>col5a3b</i>	↑ 2.6	<i>crabp2a</i>	↑ 2.1	<i>mta1</i>	↑ 1.2
<i>dpp4</i>	↑ 2.5	<i>lhx2a</i>	↑ 2.1	<i>jazf1a</i>	↑ 1.2
<i>adamts16</i>	↑ 2.5	<i>ptprt</i>	↑ 2.1	<i>erbb3b</i>	↑ 1.1
<i>lama5</i>	↑ 2.5	<i>evx1</i>	↑ 2	<i>ptk7a</i>	↑ 1
<i>col4a5</i>	↑ 2.5	<i>ablim3</i>	↑ 2	<i>elov1b</i>	↑ 1.2
<i>adamts12</i>	↑ 2.4	<i>grem1b</i>	↑ 2	<i>osbp10</i>	↑ 1.1
<i>col12a1b</i>	↑ 2.2	<i>glis1b</i>	↑ 1.9	<i>gpt</i>	↑ 1.9
<i>npr2</i>	↑ 1.9	<i>efnb3a</i>	↑ 1.7	<i>nt5c211</i>	↑ 3.7
<i>efnb3a</i>	↑ 1.7	<i>vangl1</i>	↑ 1.3	<i>slc35d3</i>	↑ 4.7
<i>col4a6</i>	↑ 1.7	<i>daam1b</i>	↑ 1	<i>rsg6</i>	↑ 4
<i>mmp16</i>	↑ 1.6	<i>hapln1b</i>	↑ 1.9		
<i>cdh6</i>	↑ 1.5	<i>irx1a</i>	↑ 1.9		
<i>nck2a</i>	↑ 1.3	<i>gdf10a</i>	↑ 2.2		
<i>FBN3</i>	↑ 1.2	<i>rdh12l</i>	↑ 2.3		
<i>col5a2</i>	↑ 1	<i>gata-1</i>	↑ 2.6		
<i>tubb5</i>	↑ 1.4	<i>crabp1b</i>	↑ 2.7		
<i>itih5</i>	↑ 2.3	<i>klf1</i>	↑ 3.4		
<i>syt9b</i>	↑ 4.3	<i>dmrt2a</i>	↑ 3.4		
<i>fscn1b</i>	↑ 1.5	<i>cecr1b</i>	↑ 3.5		
<i>tspan3a</i>	↑ 3.6	<i>slc4a1a</i>	↑ 3.7		
<i>chd</i>	↑ 2.8	<i>zic1</i>	↑ 3.9		
<i>nr2f1a</i>	↑ 1.7	<i>zic4</i>	↑ 4.3		

- Pigmentation
- Proliferation
- Metabolism
- Differentiation
- Cell-microenvironment interaction
- Dopamine homeostasis
- Immune response
- PPAR/RXR activation

↑ Highly expressed in xanthoerythrophoroma

↑ Highly expressed in melanoma